

## Researches on Modeling of Nuclear Power Plants for Dynamic Response Analysis

M. Watabe

*Building Research Institute, Ministry of Construction, Tachihara-1, Oho-cho, Tsukuba-Gun, Ibaraki, Japan*

R. Fukuzawa, O. Chiba, T. Toritani

*Nuclear Power Division, Toda Construction Company, 1-7-1, Kyobashi, Chuo-ku, Tokyo, Japan*

### SUMMARY

The dynamic response analysis has been utilized to evaluate the safety margin of nuclear power plants against major earthquakes. On modeling for the dynamic response analysis due to the horizontal component of earthquake ground motions, a large number of papers have been presented so far. For the simpler aseismic design of equipments and pipings, the dynamic response analysis due to the vertical component has been required, but very few have been related to. In this paper, authors tried to establish the rational and economical model due to the vertical component considering the dynamic soil-structure interaction effects and the flexibility of the mat foundation.

In this research, the following three types of model were introduced.

#### 1) Finite element model

Two cases of response analyses due to harmonic excitations with the finite element model were performed in which the mat foundation was treated rigid and elastic body. The dynamic soil-structure interaction effects were evaluated based on the condition that soil was semi-infinite elastic medium.

#### 2) Sophisticated mass-spring-dashpot model

Two cases of response analyses due to harmonic excitations were performed to simulate the dynamic characteristics of the finite element models mentioned above using the sophisticated mass-spring-dashpot model, in which the dynamic soil-structure interaction effects were evaluated with the same procedure applied to the finite element model.

#### 3) Simplified mass-spring-dashpot model

There were introduced three types of the simplified mass-spring-dashpot model in which the dynamic soil-structure interaction effects were simplified. Response analyses due to harmonic excitations and earthquake ground motions were performed in order to establish the rational and economical model.

It was revealed that the evaluation of the dynamic soil-structure interaction effects and the flexibility of the mat foundation had significant influence on the floor response spectra which were required for the simpler aseismic design of equipments and pipings. The simplified model could be available to estimate the maximum response values of the structure with allowable difference but should not be used to estimate the floor response.

## 1. Introduction

The dynamic response analysis has been utilized to evaluate the safety margin of nuclear power plants against major earthquakes. On modeling for the dynamic response analysis due to the horizontal component of earthquake ground motions, a large number of papers have been presented so far. For the simpler aseismic design of equipments and pipings, the dynamic response analysis due to the vertical component has been required, but very few have been related to. It has been pointed out that the evaluation of the soil-structure interaction effects plays an important role for the dynamic response analysis of nuclear power plants due to realistic earthquake ground motions, but the influence on the dynamic response analysis by evaluating the flexibility of the mat foundation has not been revealed yet. In spite that some complex problems remain, the dynamic soil-structure interaction effects are evaluated based on the condition that soil is semi-infinite elastic medium. The finite element analysis procedure which evaluates the flexibility of the mat foundation and the soil-structure interaction effects is well suited for the dynamic response analysis, however this calculation is rather time consuming in computer.

When the aseismic design of nuclear power facilities is performed in practice, the dynamic response analysis is repeatedly used under various conditions. Therefore, the development of the rational and economical model for the dynamic response analysis is expected.

The purpose of this paper is to establish the rational and economical model of nuclear power plants due to the vertical component of earthquake ground motions considering the dynamic soil-structure interaction effects and the flexibility of the mat foundation. [1]

## 2. Finite element model

Two cases of response analyses due to harmonic excitations with finite element model in which the mat foundation was treated as rigid and elastic body were performed in order to examine the influence on the dynamic response analysis by evaluating the flexibility of the mat foundation. The structure employed in this research was B.W.R. MARK II modified as shown in Fig.1 and was modeled under the assumption that the plan was symmetric with respect to two orthogonal axes. In the case of elastic body, the stiffness of the mat foundation was evaluated with 4 node shell elements shown in Fig.2, in which each nodal point had 3 degrees of freedom for a vertical displacement and two rotational angles. In the case of rigid body, the mat foundation was assumed to be a single degree of freedom for a vertical displacement. As shown in Fig.3, the structure was consisted of the shield wall, the inner wall, the outer wall, the cross wall, the floor slabs and the roof slab, and was evaluated with the same procedure applied to the mat foundation in elastic body. The damping matrix for the structure was evaluated as complex stiffness of hysteresis damping with 5 % for reinforced concrete members and with 2 % for steel ones. As the soil conditions, the following values were employed, i.e., shear velocity  $V_s=1000$  m/sec, poisson ratio  $\nu=0.4$ , density of weight  $\rho=2.0$  t/m<sup>3</sup>.

The dynamic soil-structure interaction effects were evaluated based on the condition that soil was semi-infinite elastic medium. Employing the cylindrical coordinate system  $(r, \theta, z)$  shown in Fig.4, the vertical displacement  $w(r_o, r)$  on the contact surface excited by harmonic loading  $(pe^{i\omega t})$  uniformly distributed over the circular disk of radius  $r_o$  is expressed as follows. [2]

$$w(r_o, r) = -\frac{r_o p e^{i\omega t}}{G} \int_0^\infty \frac{\sqrt{\xi^2 - \gamma^2}}{F(\xi)} J_0(\xi a) J_1(\xi a_o) d\xi \quad (1)$$

$$F(\xi) = (2\xi^2 - 1)^2 - \sqrt{\xi^2 - \gamma^2} \sqrt{\xi^2 - 1}, \quad \gamma = \sqrt{(1-2\nu)/2(1-\nu)}, \quad a_0 = r_0 \omega / V_s, \quad a = r \omega / V_s$$

in which,  $G$ ; shear moduli,  $\omega$ ; circular frequency,  $J$ ; Bessel function.

The vertical displacement  $w(r_0, r)$  excited by point loading ( $Pe^{i\omega t}$ ) is expressed as follows.

$$w(r_0, r) = -\frac{Pe^{i\omega t}}{2\pi G r} \int_0^\infty \frac{a\xi \sqrt{\xi^2 - \gamma^2}}{F(\xi)} J_0(\xi a) d\xi \quad (2)$$

The displacement excited by harmonic loading distributed over the contact area ( $S$ ) between the mat foundation and the soil is expressed by Green function.

$$w(x_1, y_1) = \int_S G(x_1, y_1 | x_2, y_2) q(x_2, y_2) dx_2 dy_2 \quad (3)$$

in which,  $w(x_1, y_1)$ ; the displacement at the cartesian coordinate  $(x_1, y_1)$ ,  $q(x_2, y_2)$ ; the distributed loading on the region  $S$ ,  $G(x_1, y_1 | x_2, y_2)$ ; Green function. [3]

In the case of elastic body, the region  $S$  was subdivided into some elements having equivalent area with rectangular elements shown in Fig.2 and each nodal point was located at the center of circular element. The integration of eq.3 was substituted approximately by the sum of eq.1 and eq.2. The relation between displacements and loads over the contact area was expressed by the matrix form, employing eq.1 for diagonal coefficients and eq.2 for off-diagonal coefficients. In the case of rigid body, it was assumed that all of the displacements over the contact area were equalized.

The distributions of the contact stress at 0 Hz in rigid body and at 8 Hz in elastic body are shown in Fig.5(a) and (b), respectively. In the case of rigid body, the distribution of the contact stress was similar to Boussinesq distribution at any frequency. In the case of elastic body, the distribution showed the very complicated shape and quite different from that in rigid body. The distribution of phase angle was almost uniform at any frequency in rigid body while in elastic body showed the varied shapes at some frequency as shown in Fig.5(c).

Frequency-responses of displacement and acceleration at the mat foundation are shown in Fig.6. The amplitude of displacement in rigid body had the maximum peak value at around 3 Hz, on the other hand in elastic body, the amplitude of each nodal points had the different peak value and then the frequencies at the maximum peak values were different. The magnification factor of acceleration in rigid body had the maximum peak value at around 4 Hz, on the other hand in elastic body, the magnification factor of each nodal point showed the similar shape of the amplitude of displacement in low frequencies and very complicated shape in higher frequencies than 7 Hz. The distributions of displacement, acceleration and their phase angles at 8 Hz in elastic body are shown in Fig.7. These figures showed that response values were different among the nodal points at the mat foundation in elastic body. Frequency-responses of displacement and acceleration at the nodal point "S", the top of the shield wall illustrated in Fig.3, are shown in Fig.8(a) and (b), respectively. Both the maximum peak values of displacement and acceleration in rigid body were larger than those in elastic body, and the frequencies at the maximum peak values in rigid body were higher than those in elastic body. The differences in response values among the nodal points at the top of each wall were smaller than those at the mat foundation.

From these results obtained, it was revealed that the influence on the frequency-response in the finite element model by evaluating the flexibility of the mat foundation should not be neglected.

### 3. Sophisticated mass-spring-dashpot model

The sophisticated mass-spring-dashpot models to simulate the dynamic characteristics of finite element models in Sec.2 were introduced. As shown in Fig.9, the structure was idealized with mass-spring-dashpot model based on the results obtained by the finite element models. In the case of elastic body, the mat foundation was treated as the beam element. The nodal points which were located at the same height of the wall were concentrated to a single nodal point. The stiffness related to axial load of each wall was evaluated as spring constant by the interpretation that all of the cross sections were effective, and then the shear stiffness of the cross wall was evaluated. The floor and roof slab were treated as the beam element. The mass was lumped at each nodal point. The damping matrix was evaluated with the same procedure in previous section.

The dynamic soil-structure effects were evaluated with the same assumption applied to the finite element model. The contact area between the mat foundation and the soil was divided into circular disk and ring shown in Fig.10 so that the sharing area of each wall was equalized to the sharing area in the finite element model. The vertical displacement  $w_{ij}$  of the center on  $j$ -th element excited by harmonic loading uniformly distributed over the  $i$ -th element is expressed as follows, applying eq.1.

$$w_{ij} = w(r_{i2}, r_j) - w(r_{i1}, r_j) \quad (4)$$

where,  $r_{i1}$  and  $r_{i2}$  are the inner and outer radius of  $i$ -th element, respectively.  $r_j$  is the mid radius of  $j$ -th element. In the case of rigid body, all of the displacements were assumed to be equalized.

The comparisons of frequency-response of acceleration between the finite element models and the sophisticated models at the mat foundation and the top of the shield wall in rigid and elastic body are shown in Fig.11 and 12, respectively. By these figures, it was revealed that the dynamic characteristics of the finite element models could be simulated by the sophisticated models.

The response analyses due to the vertical component of earthquake ground motions were performed by these sophisticated models. 10 simulated earthquake ground motions of S1 (maximum possible) were employed as input. [4] They were generated in computer to fit the response spectrum of magnitude 7 with epicentral distance 20 Km. [5] [6] Fitting status to the target spectrum is shown in Fig.13. As the average of the maximum response values are shown in Fig.14, the differences between rigid and elastic body at the top of walls were in small range from 7 to 9 %. The average of floor response spectra with 1 % damping between rigid and elastic body at the mat foundation and the top of the shield wall are shown in Fig.15. The floor response at the mat foundation in rigid body were generally smaller than that in elastic body except around 0.11 sec., on the other hand the floor response at the top of the shield wall in rigid body at around 0.11 sec. was significantly larger than that in elastic body. From these results, it was found that the influences on the maximum response values of the structure by evaluating the flexibility of the mat foundation could be neglected while on the floor response significant.

### 4. Simplified mass-spring-dashpot model

Three types of mass-spring-dashpot model with the simplified dynamic soil-structure interaction effects were introduced and the response analyses due to harmonic excitations and

earthquake ground motions were performed in order to establish the rational and economical model, that is, rather simpler analytical model in which the soil-structure interaction effects and the flexibility of the mat foundation were considered and the time consuming in computer could be saved. The complex stiffnesses of soil which represent the soil-structure interaction effects of the simplified model employed are illustrated in Fig.16.

Model 1 was the same model as the sophisticated model of elastic body mentioned in Sec.3 and was treated as the standard model. In Model 2, the mat foundation was treated as elastic body. The interaction effects of soil was evaluated with the spring constant and the equivalent damping coefficients obtained by complex stiffness. The real part of complex stiffness was the static stiffness. The imaginary part represented the dissipation in proportion to the frequency and was obtained at the fundamental frequency of the soil-structure interaction system. The interaction effects of soil connected to the nodal points at the mat foundation were obtained by dividing the complex stiffness of rigid body in proportion to the ratio of sharing area of a circular disk and rings shown in Fig.10. In Model 3, the mat foundation was treated as elastic body. The interaction effects of soil was evaluated with the spring constant and the constant equivalent damping ratio. The interaction effects of soil connected to the nodal points at the mat foundation were obtained by the same procedure in Model 2. In Model 4, the mat foundation was treated as rigid body in Model 3, therefore, this model could be defined the most simplified model. In this paper, Model 2, 3 and 4 were termed as the simplified models.

The results by frequency-response of acceleration at the mat foundation and the top of the shield wall are shown in Fig.17(a) and (b). Both magnification factors at the mat foundation and the top of the shield wall of the simplified model were rather smaller than those of Model 1 in low frequencies, and in high frequencies those of Model 3 and 4 were quite smaller. The maximum peak values of the simplified models except the top of Model 4 were smaller than those of Model 1 and the frequencies at the maximum peak values except the top of Model 2 were different from that of Model 1. From these results obtained, it was found that the simplified models could simulate the magnification factors of acceleration of Model 1 in the low frequency range but not in the high one.

The response analyses due to 10 simulated earthquake ground motions employed in Sec.2 were performed. The average of the maximum response values of acceleration are shown in Fig.18. The differences of simplified models to Model 1 at the mat foundation were within the small range while at the top of wall rather large. The maximum differences of simplified models to Model 1 at the top of walls were 13 % at the shield wall in Model 2, 25 % at the inner wall in Model 3 and 19 % at the inner wall in Model 4. The maximum difference of the simplified models to Model 1 at the center of the roof was 13 % in Model 3. From the results obtained, it was found that the simplified models could simulate the maximum response values with allowable difference. The average of floor response spectra with 1 % damping normalized by Model 1 at the mat foundation and the top of the shield wall are shown in Fig.19(a) and (b), respectively. Both response spectra at the mat foundation and the top of the simplified models were generally smaller than those of Model 1 except around 0.11 sec. The simplified model showed the tendency to underestimate the floor response in the short period range that has significant influence on the aseismic design of equipments and pipings. From these results obtained, it was found that the simplified models could not estimate the floor response spectra because of their underestimate.



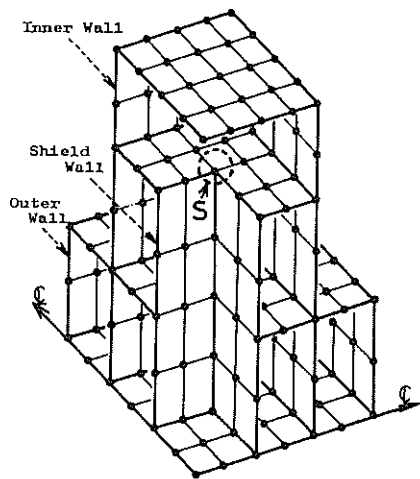
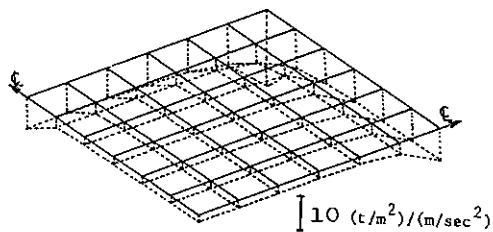
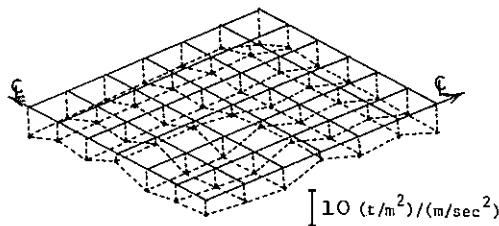


Fig.3 Finite Element Model of the Structure



(a) Amplitude in Rigid Body ( $f=0$  Hz)



(b) Amplitude in Elastic Body ( $f=8$  Hz)

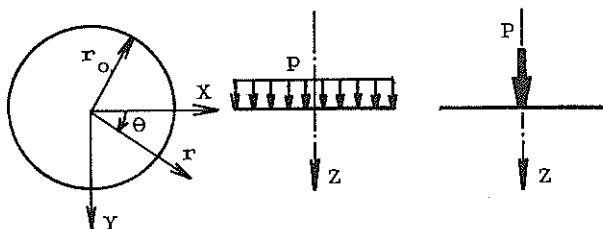
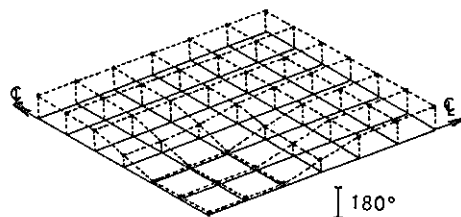
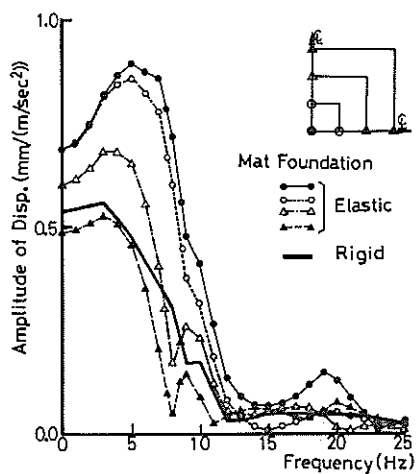


Fig.4 Cylindrical Coordinate System

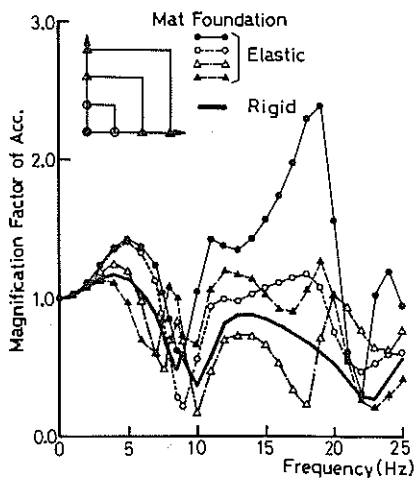


(c) Phase Angle in Elastic Body ( $f=8$  Hz)

Fig.5 Distribution of Contact stress

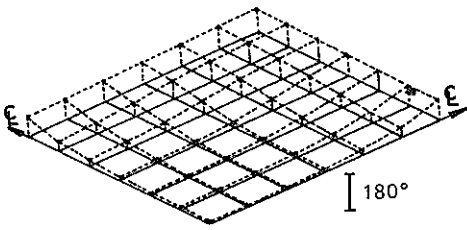


(a) Displacement

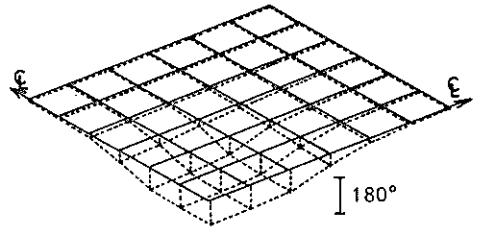


(b) Acceleration

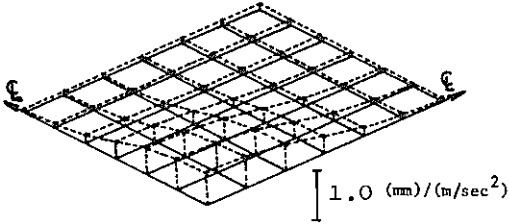
Fig.6 Frequency-Response at the Mat Foundation



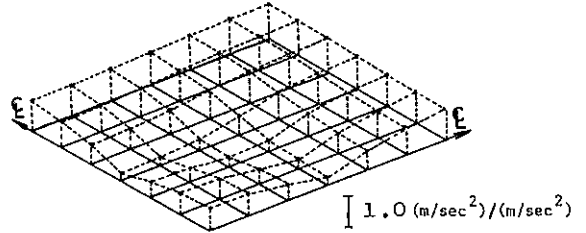
(b) Phase Angle of Displacement



(d) Phase Angle of Acceleration

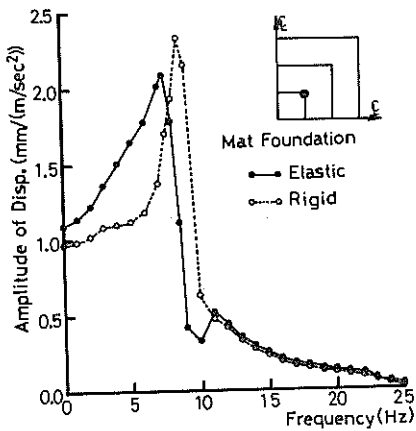


(a) Amplitude of Displacement

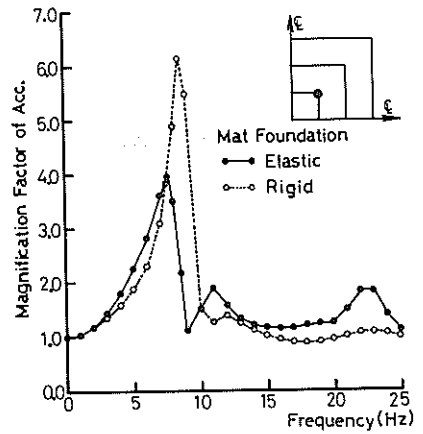


(c) Amplitude of Acceleration

Fig.7 Distribution of Displacement and Acceleration in Elastic Body ( $f=8$  Hz)



(a) Displacement



(b) Acceleration

Fig.8 Frequency-Response at the Top of the Shield wall

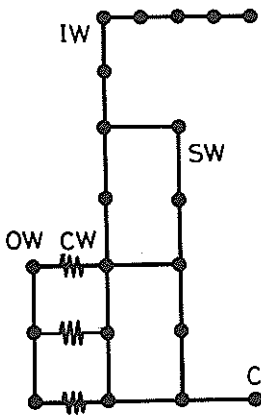


Fig.9 Mass-Spring-Dashpot Model (Sophisticated Model)

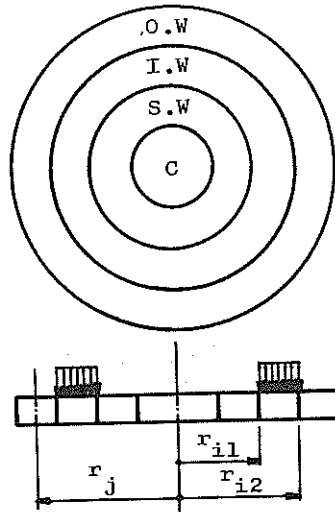
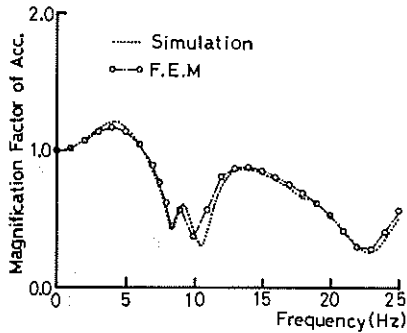
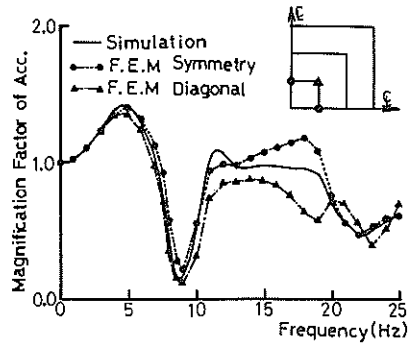


Fig.10 Equalized Contact Areas



(a) Rigid Body



(b) At the Shield Wall in Elastic Body

Fig. 11 Frequency-Response of Acceleration at the Mat Foundation

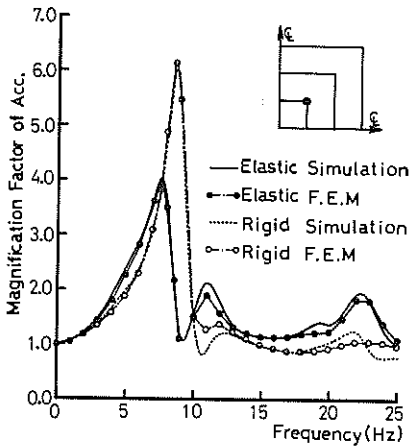


Fig. 12 Frequency-Response of Acceleration at the Top of the Shield Wall

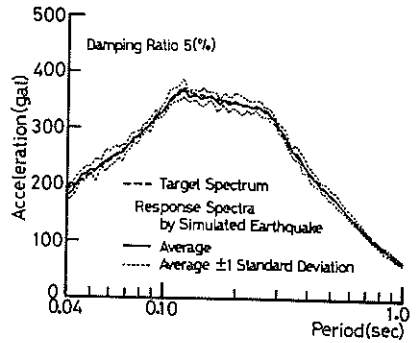
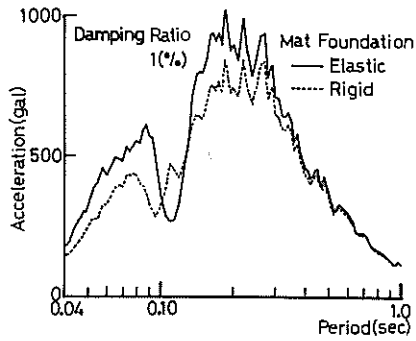


Fig. 13 Fitting Status to Target Spectrum



(a) At the Mat Foundation of the Shield Wall

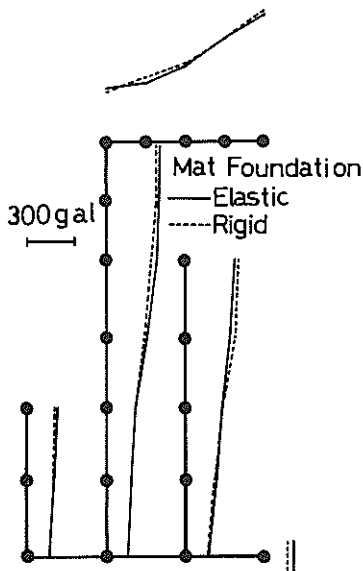
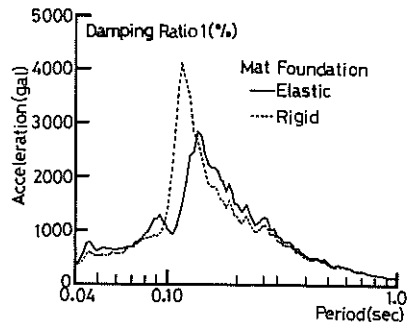


Fig. 14 Average of the Maximum Response Values of Acceleration



(b) At the Top of the Shield Wall

Fig. 15 Average of the Floor Response Spectra

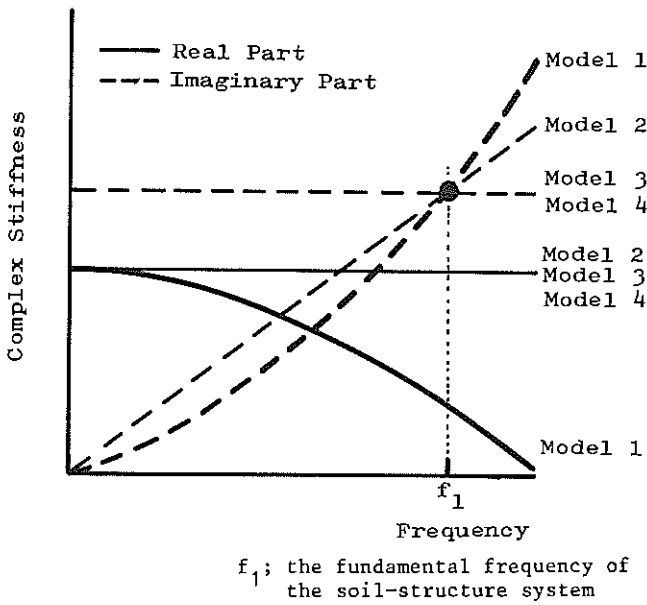


Fig. 16 Complex Stiffnesses of Soil in Rigid Body

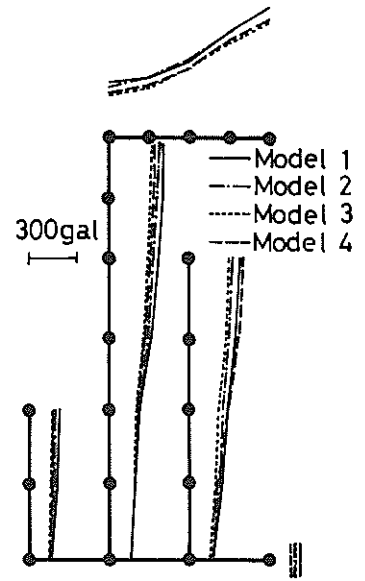
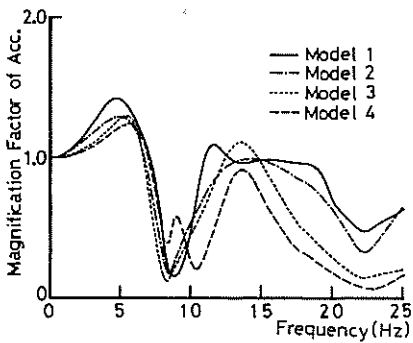
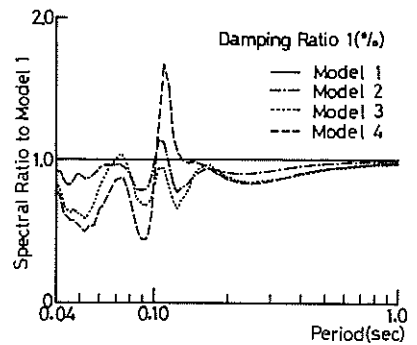


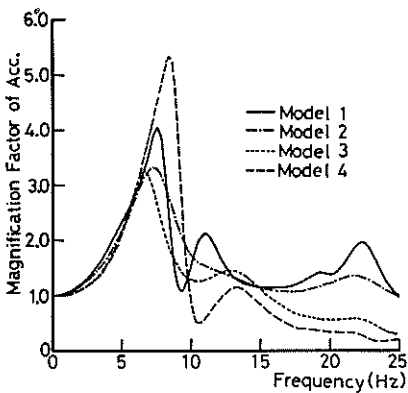
Fig. 18 Average of the Maximum Response values of Acceleration



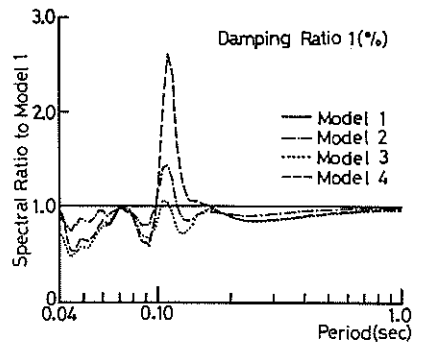
(a) At the Mat Foundation of the Shield Wall



(a) At the Mat Foundation of the Shield wall



(b) At the Top of the Shield Wall



(b) At the Top of the Shield Wall

Fig. 17 Frequency-Response of Acceleration

Fig. 19 Average of the Floor Response Spectra Normalized by Model 1